White blood cell segmentation using morphological operators and scale-space analysis

Leyza Baldo Dorini Rodrigo Minetto Neucimar Jerônimo Leite
Unicamp - Universidade Estadual de Campinas
Instituto de Computação
Caixa Postal 6176, 13083-971, Campinas, SP, Brasil
{ldorini, rodrigo.minetto}@students.ic.unicamp.br neucimar@ic.unicamp.br

Abstract

Cell segmentation is a challenging problem due to both the complex nature of the cells and the uncertainty present in video microscopy. Manual methods for this purpose are onerous, imprecise and highly subjective, thus requiring automated methods that perform this task in an objective and efficient way. In this paper, we propose a novel method to segment nucleus and cytoplasm of white blood cells (WBC). WBC composition of the blood provides important information to doctors and plays an important role in the diagnosis of different diseases. We use simple morphological operators and explore the scale-space properties of a toggle operator to improve the segmentation accuracy. The proposed scheme has been successfully applied to a large number of images, showing promising results for varying cell appearance and image quality, encouraging future works.

1 Introduction

Cell segmentation is a complex and challenging task. Cells can overlap each other, have large variation in shape and size, and be influenced by the external environment. Also, due to illumination inconsistencies, the contrast between the cell boundary and the background varies, and is different depending on the image capture conditions.

In this paper, our focus is the segmentation of white blood cells (WBC), also called leukocytes [1]. WBC are cells of the immune system, and are found throughout the body, including bone marrow and blood. Since the number of WBC in the blood is often an indicator of some diseases, the count of different classes of WBC, named differential counting, plays a major role in the determination of the patient health in different stages: diagnosis, treatment and follow up [20, 1].

WBC are classified according to their maturation levels, during what the cells can change shape, for example. Therefore, an accurate segmentation is essential for the success of subsequent high-level tasks, such as tracking and classification. Besides being very tedious and time consuming, the traditional manual method for an expert to achieve the differential counting is imprecise, hard to reproduce and subjective, being dependent of the person performing the count. Thus, automated differential counting systems is preferred.

Here, we propose an unsupervised automated segmentation method to segment WBC into the morphological components nucleus and cytoplasm. We carried out tests on a large number of images of different classes and difficult levels, like images with several cells, cells with multiple nucleus and containing a complicated background with red blood cells (RBC). We derived an efficient and robust scheme based on well-known morphological concepts, such as watershed transform and granulometric analysis.

To avoid leaking, a common problem in cell images due to the low contrast between nucleus, cytoplasm and background, we used a scale-space toggle operator for contour regularization. This shows the importance of the multiscale analysis, where it is possible to work on different representation levels to extract the specific interest features. Also, unlike several previous approaches, we do not use prior knowledge of color information.

The next section presents some related works, and Section 3 describes basic multiscale morphology definitions and operations. Section 4 defines a scale-space toggle operator and Section 5 describes our methodology. Finally, we show some results in Section 6 and draw some conclusions and future work perspectives in Section 7.

2. Related Works

Many automatic segmentation methods have been proposed, most of them based on local image information such as histogram, pixel intensity, discontinuity and clusters.

These techniques can be divided into two main categories: region-finding and contour-detection algorithms. Region-finding algorithms use a threshold based on the partition the gray level histogram, being computationally expensive. Contour-detection algorithms relies on the discontinuity of image intensities or texture at the object boundaries, being sensitive to noisy images. Also, due to the characteristics of cell images, where not all cell boundaries are sharp, it is difficult to extract all the edge information.

The use of thresholding techniques performs poorly in most part of the cases, since no spatial information is used during the selection of the segmentation thresholds. Sometimes, these techniques are combined with mathematical morphology operations [14].

Kumar et al. [8] segment the nucleus boundary using the Teager energy operator, obtaining very effective results. To segment the cytoplasm, they used a simple morphological method similar to that used in this paper. Theera-Umpon [20] proposes an automatic technique to segment nucleus and cytoplasm of bone marrow WBC based on the fuzzy C-means algorithm and basic mathematical morphology operations.

Liao [10] introduces the use of shape analysis into WBC segmentation, locating accurate WBC contour with a shape analysis step based on a roughly boundary obtained by thresholding. In [7] Jiang proposes a WBC segmentation scheme based on scale-space filtering and HSV histogram clustering.

Finally, several differential counting approaches are applied to peripheral blood only. But this may not be enough for diagnosis purposes where we have a high density of cells, like in the WBC images.

3. Mathematical Morphology Concepts

Mathematical morphology is a non-linear image analysis technique that extracts image object's information by describing its geometrical structures in a formal way. Since its formalization by Matheron and Serra [12] [16], [17], mathematical morphology has been largely used in several practical and theorical image processing and analysis problems.

In the following, we review briefly some mathematical morphology operators and the corresponding operations used in this work.

3.1 Multiscale Morphology

Let $f : \mathcal{D} \subset \mathbb{R}^n \to \mathbb{R}$ be an image function and $g : \mathcal{G} \subset \mathbb{R}^n \to \mathbb{R}$ be a structuring function. The two fundamental operations of gray-scale morphology, erosion and dilation, are defined as:

Definition 1 *[3] (Dilation) The dilation of the function $f(\boldsymbol{x})$ by the structuring function $g(\boldsymbol{x})$, $(f \oplus g)(\boldsymbol{x})$, is given by:*

$$(f \oplus g)(\boldsymbol{x}) = \max\{f(\boldsymbol{z}) + (g_{\boldsymbol{x}})(\boldsymbol{z}) : \boldsymbol{z} \in \mathcal{D}[g_{\boldsymbol{x}}]\} \quad (1)$$

Definition 2 *[3] (Erosion) The erosion of the function $f(\boldsymbol{x})$ by the structuring function $g(\boldsymbol{x})$, $(f \ominus g)(\boldsymbol{x})$, is given by:*

$$(f \ominus g)(\boldsymbol{x}) = \min\{f(\boldsymbol{z}) - (g_{\boldsymbol{x}})(\boldsymbol{z}) : \boldsymbol{z} \in \mathcal{D}[g_{\boldsymbol{x}}]\} \quad (2)$$

where $g_{\mathbf{x}}$ indicates the translation by $\mathbf{x}$ $(g_{\mathbf{x}})(\mathbf{z}) = g(\mathbf{z} - \mathbf{x})$, and $\mathcal{D}[g_{\mathbf{x}}]$ denotes the domain of the translated structuring function.

The result of these two operations depends on the location of the structuring function center. To avoid level-shifting and horizontal translation effects, respectively, one must consider that $\sup_{\mathbf{t}\in\mathcal{G}}\{g(\mathbf{t})\} = 0$ and $g(\mathbf{0}) = 0$

To handle with the multiscale nature of the image data, we can perform the analysis of different representation levels and explore the specific features that become explicit at each scale. To introduce the notion of scale, we can make the above morphological operations scale dependent by defining a scaled structuring function $g_\sigma : \mathcal{G}_\sigma \subset \mathbb{R}^2 \to \mathbb{R}$ such that [6]

$$g_\sigma(\mathbf{x}) = |\sigma| g(|\sigma|^{-1}\mathbf{x}) \quad \mathbf{x} \in \mathcal{G}_\sigma,\ \forall \sigma \neq 0, \quad (3)$$

where $\mathcal{G}_\sigma = \{\mathbf{x} : \|\mathbf{x}\| < \mathcal{R}\}$ is the support region of the function g_σ [6].

To ensure reasonable scaling behavior, some other conditions are necessary [6], which require a monotonic decreasing structuring function along any radial direction from the origin. Here, we use as structuring function $g(x, y) = -\max\{x^2, y^2\}$ which in the scaled version is given by

$$g_\sigma(x, y) = -|\sigma|^{-1} \max\{x^2, y^2\}, \quad (4)$$

where σ represents the scale of the structuring function. Observe that, for a 3×3 structuring element (used in this work), g_σ is zero at position $\mathbf{0}$ and $-|\sigma|^{-1}$ otherwise.

Scaled morphological operators have been frequently associated to non-linear filters (image sharpening, for example) and scale-space theory. In this work, we explore the scale-space extrema preservation properties of a toggle transformation that uses these operators as primitives [9].

3.2. Image Segmentation by Watershed Transform

Image segmentation consists basically on partitioning an image into a set of disjoint (non-overlapping) and homogeneous regions which are supposed to correspond to image objects that are meaningful to a certain application. In a morphological framework, this is typically done by first extracting markers of the significant structures (to prevent

over-segmentation), and then using the watershed transform [2] to extract the contours of these structures as accurately as possible.

The watershed transform is a powerful segmentation tool, combining region growing and edge detection techniques to partition the image into two different sets: the catchment basis and the watershed lines [2, 19]. If an image is seen as a topographic surface, the watershed transform can be understood as a flooding process, in such a way that whenever two bodies of water from different seeds meet it forms a line (dam). When applying the watershed transform to the image gradient, the catchment basis theoretically correspond to the homogeneous gray level regions of the image.

To determine the watershed transform we used the image forest transform (IFT) [4]. The IFT defines a minimum-cost path forest in a graph, whose nodes are the image pixels and arcs are defined by an adjacency relation between pixels. The cost of a path in this graph is determined by an application-specific path-cost function, which usually depends on local image properties along the path - such as color, gradient and pixel position. For suitable path-cost functions, the IFT assigns one minimum-cost path from a given set of seed pixels to each pixel, in such a way that the union of those paths is an oriented forest, spanning the whole image.

Image segmentation is one of its most important applications of IFT, covering both boundary- and region-based paradigms. In our approach, the first step to compute the IFT-Watershed from markers [11] is to define internal and external seeds. The internal seeds must necessarily belong to the interest object, and the external ones are initialized as the edges of the original image. Based on these seeds, the IFT assigns a minimum-cost path from them to each pixel such that each seed becomes root of an optimum-path tree composed by its most strongly connected pixels [4]. The resulting optimum-path forest consists of two sub-forests with distinct labels: object and background. In this paper, the adjacency relation is defined as 8-connected neighbors.

A failure ("leaking") occurs when an object seed conquers background pixels or vice-versa. One can avoid this problem using sophisticated algorithms such as Tree-Pruning [13]. In this paper, we use a simpler approach to prevent these failures by pre-processing the input image with a scale-space toggle operator using non-flat structuring elements. In the next section, we present the definition and some interesting properties of this operator.

4. Scale-space Toggle Operator for Image Simplification

A toggle operator has two major points: the primitives and a given decision rule [19]. Here, an extensive and an anti-extensive transformation are used as primitives, namely, the scale dependent dilation and erosion. The decision rule involves, at a point $\mathbf{x}$, the value $f(\mathbf{x})$ and the primitives results. Formally [9]:

$$(f \oslash g_\sigma)^k(\mathbf{x}) = \begin{cases} \psi_1^k(\mathbf{x}) & \text{if } \psi_1^k(\mathbf{x}) - f(\mathbf{x}) < f(\mathbf{x}) - \psi_2^k(\mathbf{x}), \\ f(\mathbf{x}) & \text{if } \psi_1^k(\mathbf{x}) - f(\mathbf{x}) = f(\mathbf{x}) - \psi_2^k(\mathbf{x}), \\ \psi_2^k(\mathbf{x}) & \text{otherwise,} \end{cases} \tag{5}$$

where $\psi_1^k(\mathbf{x}) = (f \oplus g_\sigma)^k(\mathbf{x})$, that is, the dilation of $f(\mathbf{x})$ with the scaled structuring function g_σ k times. In the same way, $\psi_2^k(\mathbf{x}) = (f \ominus g_\sigma)^k(\mathbf{x})$.

This definition is similar to that of the Schavemaker's operator [15]. The main difference is that, while the latter performs one dilation and one erosion in each iteration, the above defined operator performs k erosions and dilations, and then makes the comparison. Also, this operator is applied once and, depending on the application, uses higher structuring elements.

To avoid undesirable effects such as halos and oscillations, idempotent toggle operators are used [18]. Although the toggle operator defined in Equation 5 is not idempotent, it has a well-controlled behavior, since it uses an alternative solution to this problem based on the specific knowledge of the pixels transformation.

Leite and Dorini [9] proved that a pixel can initially converge to a specific local minimum and, after a certain iteration, to converge to an image maximum, or vice-versa. Furthermore, the sequence is stationary, which implies that it converges to a constant value, that is, it stabilizes after a certain number of iterations.

In other words, the pixel belongs to a single influence zone, for all the iterations, or is affected by an influence zone of a stronger image extrema of the same class (maximum or minimum). At this way, in some neighborhood of an important minimum (maximum), the pixels values will be eroded (dilated) so that it is possible to identify the significant extrema of the image and their influence zones through a simple thresholding operation that uses a decision rule similar of that in Equation 5, given by:

$$(f \oslash g_\sigma)^k(\mathbf{x}) = \begin{cases} 255 & \text{if } \psi_1^k(\mathbf{x}) - f(\mathbf{x}) <= f(\mathbf{x}) - \psi_2^k(\mathbf{x}) \\ 0 & \text{otherwise} \end{cases} \tag{6}$$

where, again, $\psi_1^k(\mathbf{x}) = (f \oplus g_\sigma)^k(\mathbf{x})$, that is, the dilation of $f(\mathbf{x})$ with the scaled structuring function g_σ k times. In the same way, $\psi_2^k(\mathbf{x}) = (f \ominus g_\sigma)^k(\mathbf{x})$.

In this paper, we explore some interesting scale-space properties of the operator defined by Equation 5, concerning mainly image extrema preservation according to the strong monotonicity property. Since new extrema are created across scales, we have a well-controlled extrema merging behavior that also preserves the main geometric features of the image.

We also investigate the use of iterative applications of this operator, simplifying the image in such a way that edges are regularized, improving the quality of the image gradient and yielding better segmentation results. Furthermore, with scale-space operators it is possible to relate information obtained in different representation levels, as well as to have a precise localization of the interest features in the original signal.

5. Proposed Technique for WBC Segmentation

A typical blood smear image has three main classes of objects, namely, background, RBC and WBC. In the following, we discuss our approach to segment the WBC into nucleus and cytoplasm.

In contrast to several other approaches that require one sub-image for each WBC, our scheme also obtain sound segmentation results for images composed by several WBC, even on complicated backgrounds containing overlapping RBC. In a first step, we extract the cell nucleus using the watershed transform by IFT. Then, we explore the size distribution information of the RBC to segment the WBC cytoplasm using basic operations such as thresholding and morphological opening. We discuss the complete approach below.

5.1. Nucleus Segmentation

For nucleus segmentation, we use the watershed transform by IFT, a general tool for the design of image processing operators based on connectivity (Section 3.2). Since the shape of the WBC nucleus is extremely important in several further tasks, such as classification for differential counting purposes, we use a path-cost function that takes into account suitable image characteristics.

To prevent over-segmentation, it is necessary to choose an initial set of internal seeds in such a way that only the interest objects are marked. Since WBC nucleus is darker than the rest of the image, we just perform a thresholding to obtain (at least) one sample of each WBC (we used 90 as threshold value for all tests).

Due to illumination inconsistencies, the contrast between the nucleus and cytoplasm boundaries can change significantly, implying a weak gradient image. Thus, its use as external seed can cause a leaking in the resulting segmentation. There are some extensions of the watershed by IFT to avoid this problem, such as Tree Prunning [13], which previously identify leaking pixels.

For our WBC image set it was not necessary to use such sophisticated techniques. To prevent leaking, we perform iterative applications of the operator defined in Equation 5 at a suitable scale. This procedure creates a simplified image having a homogeneous distribution on the gray levels, which leads to a contour regularization that improves the quality of the gradient image. This behavior is explained by the scale-space and convergence properties of the operator. In this paper, we consider 10 iterations at scale one for most part of the tests.

Figure 1 illustrates this improvement. Note that the gradient extracted from the original image is weak, that is, it does not necessarily have higher values on boundary pixels, which causes a leaking. The contour regularization obtained in the image processed with the operator (Equation 5) has a quality superior than when tradicional methods like high-boost and Laplacian [5] are used. Also, this scheme can be applied to noisy images, since the simplification performs a filtering in the original image, while preserving and enhancing the boundaries.

Finally, since the cell nucleus is not sharp, it is necessary to discard small regions connected to the nucleus that correspond to cytoplasm pixels. For this, we compute an erosion (of size one) on the image processed by the operator defined in Equation 5. The proposed nucleus segmentation scheme is summarized in the Algorithm 1 below.

Algorithm 1 Nucleus segmentation procedure

1: **function** WBC NUCLEUS SEGMENTATION SCHEME
2: given an input image I;
3: create a binary image, Ib, by thresholding;
4: create a simplified image, Is, applying Eq. 5 on I;
5: compute an erosion on Is to discard small residues;
6: compute the watershed transform using Ib as markers and Is to compute the gradient;
7: **end function**

5.2. Cytoplasm Segmentation

Our approach to cytoplasm segmentation explores the size distribution information of the blood smear images. As we have already segmented the nucleus, our aim is to separate cytoplasm from background and RBC. Since RBC have a similar size, generally small than that of the WBC, we can use this information to discard them.

A powerful morphological tool which captures the size distribution of spatial observations are the granulometries, introduced by Matheron [12]. One way to obtain a granulometric function is by performing a series of morphological openings using structuring elements of increasing size. Thus, we have a mapping between structuring element size and number of removed image objects.

In a first step, we threshold the original image separating background from objects (background is always brighter than the objects in this class of images). Then, we compute an erosion with a disk-shaped structuring element of a size grater than the size distribution of the RBC. This results

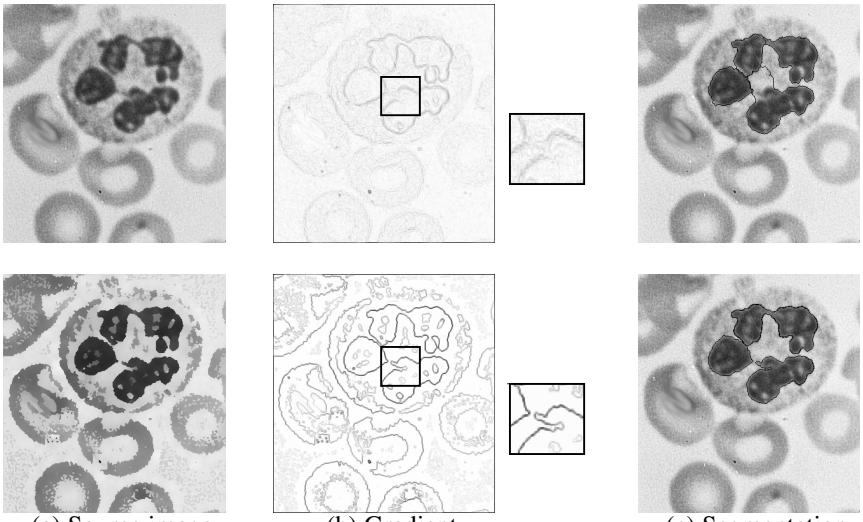

(a) Source image (b) Gradient (c) Segmentation

Figure 1. Improvement of the gradient image when applying a scale-space toggle operator.

in a set of WBC markers (the only connected components in the thresholded image that satisfy this specific size).

Finally, we perform a dilation (characterizing an opening) with a structuring element of the same size, obtaining a binary image whose boundaries correspond to an approximation of the cytoplasm. The edges of the resulting componentes are then superimposed in the original image. Another approach would consist on a morphological reconstruction using the eroded image as marker.

Some images have overlapping RBC that will correspond to a large connected component in the thresholded image, which can be misclassified as a WBC. To avoid this, we verify if the resulting connected components contain (envolves) a pre-segmented nucleus. If no, we discard the component.

This procedure presents some limitations. However, for classification purposes (our future work focus), the main component is the nucleus. The cytoplasm just helps us to differentiate between some maturation stages of the WBC (where the nucleus shape is similar, but the proportion nucleus/citoplasm is different).

The cytoplasm segmentation scheme is summarized in Algorithm 2 and illustrated in Figure 6.

Algorithm 2 Cytoplasm segmentation procedure

1: **function** WBC CYTOPLASM SEGMENTATION SCHEME
2: given an input image I;
3: compute the granulometric function to obtain the size distribution of the RBC, sd;
4: create a binary image, Ib, using thresholding to separate background and objects;
5: compute an opening on Ib with a structuring element of size sd;
6: discard components that do not intersect with a previously segmented nucleus.
7: **end function**

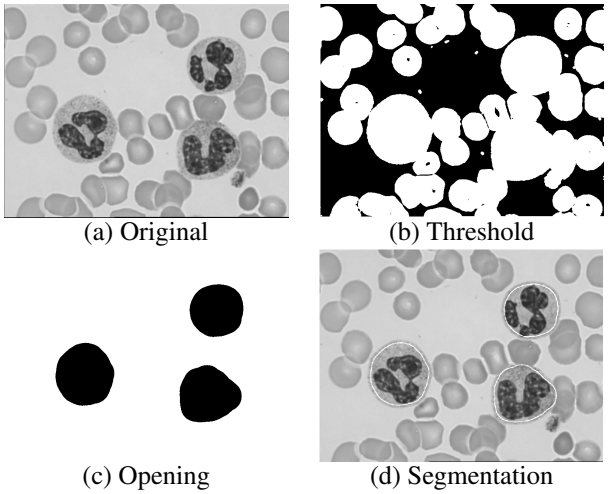

(a) Original (b) Threshold (c) Opening (d) Segmentation

Figure 2. Cytoplasm segmentation scheme.

6. Results and Discussion

In the experiments we used grayscale images from the `CellAtlas.com`[1] reference library, a public cell image database with images of human blood cells classified by experts within the field of hematology. We carried out tests on over 100 images, obtaining promising results. In the

[1] http://h34.cellavision.se/start/

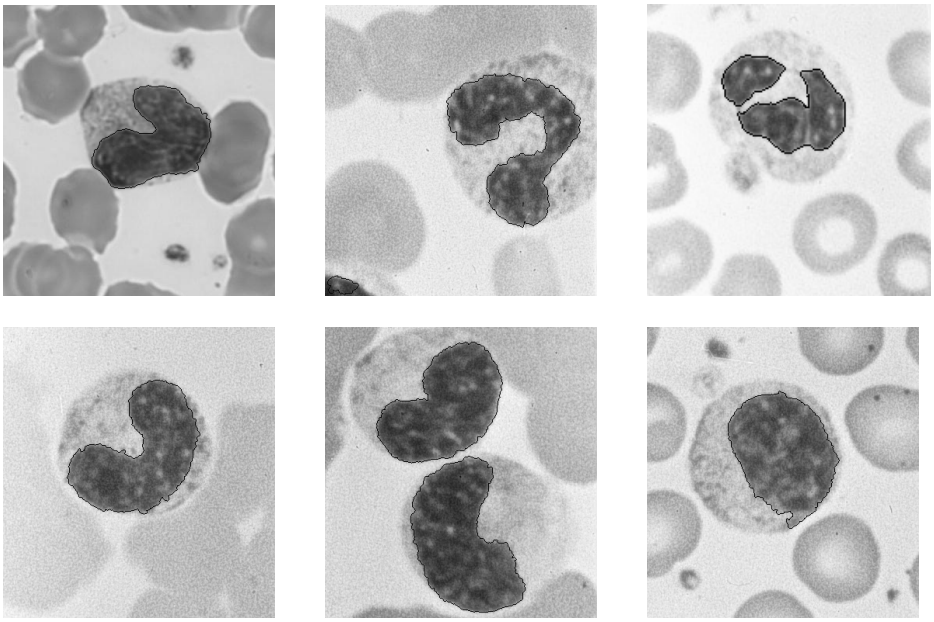

Figure 3. Nucleus segmentation results using simple images with one WBC.

following, nucleus and cytoplasm segmentation results are analyzed separately, since the nucleus shape is the most important feature for our future classification purposes.

Figure 3 shows the segmentation results for sub-images with only one WBC. Note that some images contain noise, another factor that influences the quality of the gradient image. However, besides performing contour regularization, the simplification performed by the operator (Equation 5) also filters the image, which makes our method robust to noise. Nucleus is accurately segmented for all the examples.

Figure 4 presents segmentation results for more complex images, with a complicated background and containing several WBC and RBD. There are also cells with multiple nucleus. Again, we obtained accurate segmentation results. Thus, in contrast to other approaches, it is not necessary an adicional step for sub-image extraction.

Another very important aspect is that our method is robust to leaking. Figure 5 illustrates some results where the processing of the initial image with the operator defined in 5 is crucial for a good gradient estimate and subsequent accurate segmentation.

Finally, Figure 6 illustrates some cytoplasm segmentation results. We can see that the estimate is not perfect but it can be property considered as an approximation of the cytoplasm area and shape.

7. Conclusions

We have presented a method for WBC segmentation into nucleus and cytoplasm. This is particulary important for differential counting, which helps in the diagnosis of several diseases.

Our method successfully segments WBC images into nucleus, cytoplasm and background. Another important contribution is the use of a scale-space toggle operator to regularize the image contours, leading to a better segmentation without leaking. The image simplification performed by the multi-scale operator also filter out the noise present in some images.

Although we have just performed a qualitative analysis of the results, the accurate nucleus segmentation results encourage future works which include the classification of WBC using shape descriptors extracted from segmented nucleus. The cytoplasm information will be important to classify similar shapes from different maturation levels, where the only difference between classes is the proportion between nucleus and cytoplasm areas.

References

[1] B. Alberts, A. Johnson, J. Lewis, M. Raff, K. Roberts, and P. Walter. *Molecular Biology of the Cell*. Garland Science, 2002.

[2] S. Beucher and F. Meyer. The morphological approach to segmentation: the watershed transformation. *Mathematical Morphology in Image Processing*, pages 433–1993, 1993.

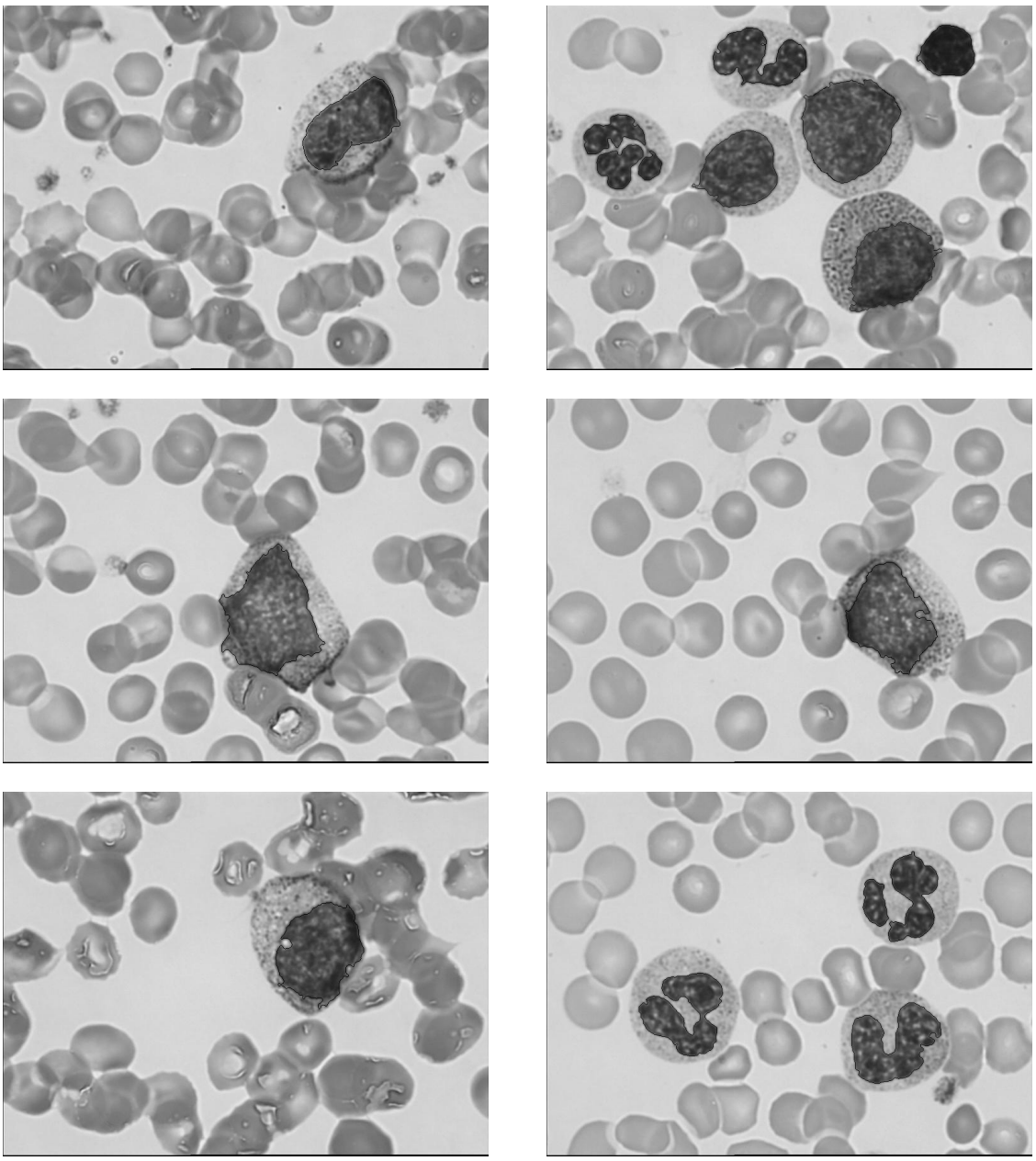

Figure 4. Nucleus segmentation results using images with several WBC.

[3] E. R. Dougherty and R. A. Lotufo. *Hands-on Morphological Image Processing*. SPIE-International Society for Optical Engine, 2003. ISBN: 081944720X.

[4] A. X. Falcão, J. Stolfi, and R. A. Lotufo. The image foresting transform: Theory, algorithms, and applications. *IEEE Trans. on Pattern Analysis and Machine Intelligence*, 26(1):19–29, Jan 2004.

[5] R. C. Gonzalez and R. E. Woods. *Digital Image Processing*. Prentice Hall Upper Saddle River, 2001. ISBN: 0-20118-075-8.

[6] P. T. Jackway and M. Deriche. Scale-space properties of the multiscale morphological dilation-erosion. *IEEE Transactions on Pattern Analysis and Machine Intelligence*, 18:38–51, 1996.

[7] K. Jiang, Q. Liao, and S. Dai. A novel white blood cell segmentation scheme using scale-space filtering and watershed clustering. In *2nd International conference on machine learning and cybernetics*, pages 2820–2825, 2003.

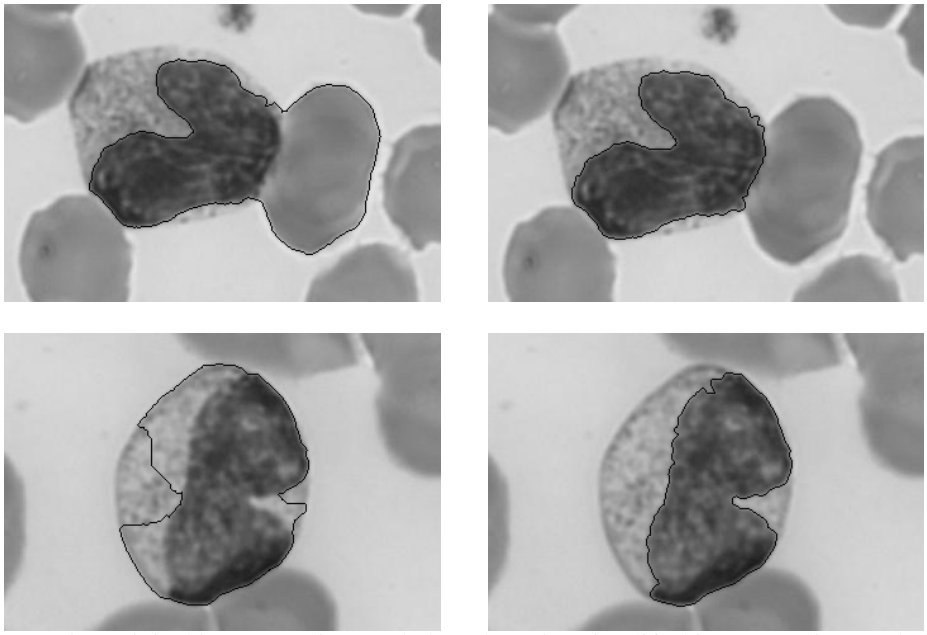

(a) Using original image gradient (Sobel) (b) Using simplified image gradient (Sobel)

Figure 5. Avoiding leaking by using an image processed by the defined scale-space operator.

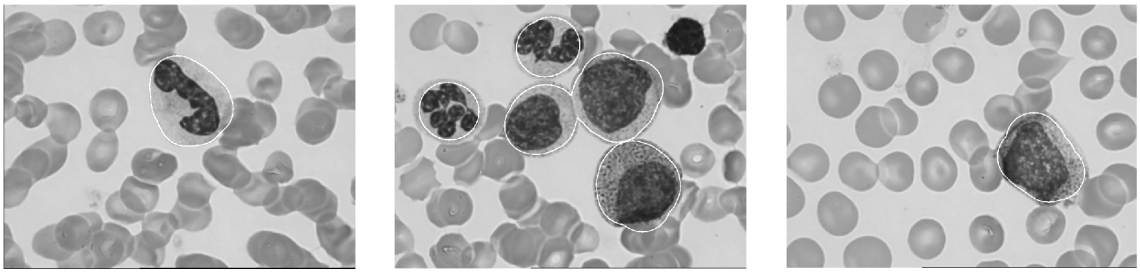

Figure 6. Some cytoplasm segmentation results.

[8] B. Kumar and T. Sreenivas. Teager energy based blood cell segmentation. In *International conference of digital signal processing*, volume 2, pages 619–622, 2002.

[9] N. J. Leite and L. E. B. Dorini. A scaled morphological toggle operator for image transformations. In *XIX Brazilian Symposium on Computer Graphics and Image Processing*, pages 323–330. IEEE Press, 2006.

[10] Q. Liao and D. Y.Y. An accurate segmentation method for white blood cell images. In *IEEE International symposium on biomedical imaging*, pages 245–248, 2002.

[11] R. A. Lotufo, A. X. Falcão, and F. Zampirolli. IFT-Watershed from gray-scale marker. In *Proc. of XV Brazilian Symp. on Computer Graphics and Image Process ing*, pages 146–152. IEEE, Oct 2002.

[12] G. Matheron. *Random Sets and Integral Geometry*. John Wiley and Sons, 1975.

[13] P. Miranda, F. Bergo, L. Rocha, and A. Falcão. Tree-pruning: A new algorithm and its comparative analysis with the watershed transform for automatic image segmentation. In *XIX Brazilian Symposium on Computer Graphics and Image Processing*, pages 231–239. IEEE Press, 2006.

[14] C. Ruberto, A. Dempster, S. Khan, and B. Jarra. Segmentation of blood images using morphological operators. In *International conference on pattern recognition*, pages 3401–3405, 2000.

[15] J. G. M. Schavemaker, M. J. T. Reinders, J. Gerbrands, and E. Backer. Image sharpening by morphological filtering. *Pattern Recognition*, 33:997–1012, 1999.

[16] J. Serra. *Image Analysis and Mathematical Morphology*. Academic Press, 1982.

[17] J. Serra. *Image Analysis and Mathematical Morphology, volume 2: Theoretical Advances.* Academic Press, 1988.

[18] J. Serra and L. Vicent. An overview of morphological filtering. *Circuits, Systems and Signal Processing*, 11(1):47–108, 1992.

[19] P. Soille. *Morphological Image Analysis: Principles and Applications*. Springer-Verlag, 2003.

[20] N. Theera-Umpon. White blood cell segmentation and classification in microscopic bone marrow images. *Lecture Notes on Computer Science*, (3614):787–796, 2005.